URSI GASS 2021, Rome, Italy, 28 August - 4 September 2021

Iterative Space-angle Discontinuous Galerkin Method for Radiative Transfer Problems from 1D to 3D

Hang Wang[(1)], Reza Abedi[(1)], and Saba Mudaliar[(2)]
(1) University of Tennessee Space Institute (UTSI), Tullahoma, TN 37388, www.rezaabedi.info, rabedi@utsi.edu
(2) Sensors Directorate, Air Force Research Laboratory, Wright-Patterson AFB, Dayton, OH 45433, saba.mudaliar@us.af.mil

Abstract

The radiative transfer equation (RTE) for problems involving scattering, absorption and radiation is solved using the space-angle discontinuous Galerkin (DG) method in multi-dimensions from 1D to 3D. The space and angle is fully discretized by the DG formulation by utilizing the element extrusion technique. Moreover, the iterative and parallel scheme is used for the solution process, making the process in a relatively cheap way.

1 Introduction

Radiative transfer takes place in a wide range of natural phenomena and engineering applications. The propagation of radiation in the form of electromagnetic waves through a medium is affected by absorption, emission, and scattering processes. The radiative transfer equation (RTE) mathematically describes this interaction, which has a wide range of applications in such areas as heat transfer, neutron transport, atmospheric science, optical molecular imaging and some other applications. In the steady state, the RTE is an integro-differential equation of up to five independent variables, which are 3 dimensions in space and 2 directions of the solid angle. The high dimensionality and the integral term present serious challenges when trying to solve the RTE numerically. The discontinuous Galerkin (DG) finite element method (FEM), introduced by Reed and Hill [1], is one of the most popular grid-based numerical methods for solving the RTE due to its high order accuracy and flexibility in mesh grids. The basis functions used in the DG method are discontinuous across element interfaces; accordingly, the jump condition between interior traces of solution and the so-called numerical flux is weakly enforced on the interface boundaries. The space-angle DG method are specially suitable for the RTE, since the evolution of solution along characteristics can be strongly discontinuous in both space and angle.

In our previous work, the RTE for plane-parallel problems and 2D axisymmetric problems are solved by the DG method directly [2, 3, 4]. However, a direct solver may end up with much higher memory usage, when dealing a higher dimensional problem, such as a 3D problem. To overcome this issue, an iterative and parallel DG solver with angular decomposition scheme is applied in this paper to solve the steady state radiative transfer problems in multi-dimensions.

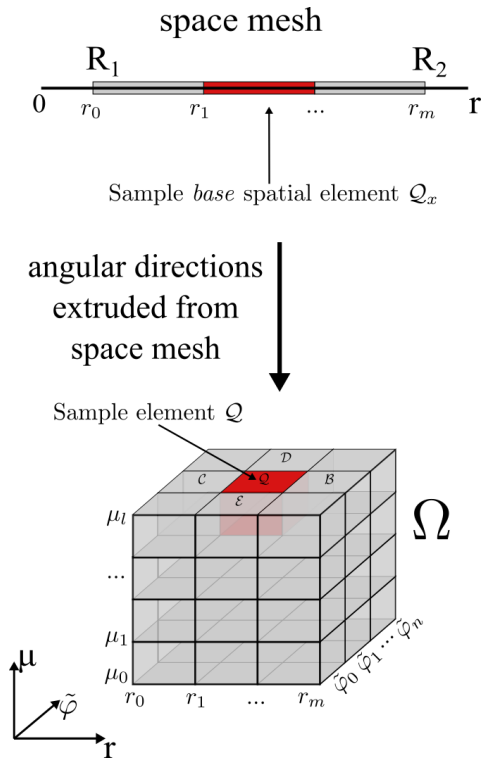

Figure 1. The illustration of the extrusion of the spatial domain in angle directions μ and $\tilde{\varphi}$. The left figure shows the one-dimensional spatial elements and the right shows their extrusion to form the three-dimensional domain Ω.

2 Radiative transfer equation

The general form of steady-state RTE for a gray medium is given as,

$$\frac{\mathrm{d}I(\mathbf{x},\hat{\mathbf{s}})}{\mathrm{d}s} = -\beta I(\mathbf{x},\hat{\mathbf{s}}) + \kappa I_b(\mathbf{x}) + \frac{\sigma_s}{4\pi}\oint_{4\pi} I(\mathbf{x},\hat{\mathbf{s}}')\Phi(\hat{\mathbf{s}},\hat{\mathbf{s}}')\mathrm{d}s' \quad (1)$$

This equation describes the change of radiation intensity $I(\mathbf{x},\hat{\mathbf{s}})$ at spatial location $\mathbf{x}$ along the path $\mathrm{d}s$ in the angle space with angle coordinate $\hat{\mathbf{s}}$. The values β, κ, and σ_s, are the spatial-dependent extinction, absorption, and scattering coefficients, respectively. The anisotropic scattering

phase function is represented by $\Phi(\hat{\mathbf{s}},\hat{\mathbf{s}}')$ and $\mathbf{s}'$ is the solid angle for phase function integration. The solid angle differential for $\mathbf{s}'$ is denoted by $\mathrm{d}s'$. The spatial-dependent total black-body radiation intensity is given by I_b. For problems in different dimensions or different coordinate systems, the left hand side term of Eqn. 1, $\mathrm{d}I(\mathbf{x},\hat{\mathbf{s}})/\mathrm{d}s$, is different. In this paper, we are focusing on the problems in 1D cylindrical coordinate and 2D and 3D Cartesian coordinate in space and 2 directions in angle.

3 DG formulation

To implement general RTEs, the software written by us supports the extrusion of a 1D to 3D spatial domain, discretized by simplicial elements, into arbitrary number of extrusions in angle. To implement general RTEs, the software written by us supports the extrusion of a 1D to 3D spatial domain, discretized by simplicial elements, into arbitrary number of extrusions in angle. Figure 1 illustrates how the space-angle mesh is generated for a 1D spatial mesh extruded in two angular directions, as an example. The 1D simplicial spatial elements (lines) on the left are extruded first to the 9 once-extruded simplicial elements (squares) in the $r-\tilde{\varphi}$ plane and next to twice-extruded simplicial elements (cubes) in Ω. The above RTE can then be discretized over a space-angle finite element domain.

In a DG formulation, residuals (errors) must be specified both in the interior and on the boundary of elements. The weighted residual (WR) of the finite element formulations formed by multiplying the RTE (Eqn. 1) by the weight function $\hat{H}$,

$$\begin{aligned}&\int_{\mathcal{Q}} \hat{H}\left[\frac{\mathrm{d}I(\mathbf{x},\hat{\mathbf{s}})}{\mathrm{d}s}+\beta I(\mathbf{x},\hat{\mathbf{s}})-\kappa I_b(\mathbf{x})\right]\mathrm{d}V\\ &-\int_{\mathcal{Q}} \hat{H}\left[\frac{\sigma_s}{4\pi}\oint_{4\pi} I(\mathbf{x},\hat{\mathbf{s}}')\Phi(\hat{\mathbf{s}},\hat{\mathbf{s}}')\mathrm{d}s'\right]\mathrm{d}V\,, \qquad (2)\\ &+\int_{\partial\mathcal{Q}} \hat{H}\,(I^*-I)\,\hat{\mathbf{s}}\cdot n\mathrm{d}A=0\end{aligned}$$

where $\mathcal{Q}$ is the element, $\partial\mathcal{Q}$ is the element boundary, n is the normal vector of the element facet. The numerical solution I used in DG method for each space-angle element $\mathcal{Q}$ is defined by $I^h_{\mathcal{Q}}=\hat{I}_{\mathcal{Q}}\cdot\mathbf{a}$, where $\hat{H}_{\mathcal{Q}}$ is the tensorial product monomials within element $\mathcal{Q}$ and $\mathbf{a}$ is the unknown vector for element $\mathcal{Q}$. The term $(I^*-I)\hat{\mathbf{s}}\cdot n$ is the jump condition which weakly enforces the continuity between each element. Each of the above terms are placed into a local stiffness and force tensor which is then transferred to a global stiffness K matrix and force $\mathbf{F}$ vector in the equation: $K\mathbf{a}=\mathbf{F}$. The unknown vector $\mathbf{a}$ can be obtained by the direct solution of this linear system.

4 Iterative and parallel implementation

Directly solving the system requires dealing a large stiffness especially for the multi-dimensional RTEs with the angular integration term. As the angular decomposition (AD) is applied, meaning the space-angle domain is sliced along the angle direction and divided into several sub-domains, each sub-domain can be solved separately. The the global stiffness is then split into $K=A+B$, where A is the global matrix from sub-domain stiffness and B is the stiffness contributions by the angular integration term in Eqn. 2. Instead of solving $K\mathbf{a}=F$, A is used as the approximate stiffness, and B is moved to the right hand side, $A\mathbf{a}=F-B\mathbf{a}$. This significantly reduces the degrees of freedom within a slab and makes the stiffness sparser. For example, Figure 2 shows the sparsity patterns of a global stiffness and sub-domain stiffness matrices. Subsequently, the domain is solved iteratively by updating the solution of each sub-domain until the residuals of the solution R_n at step n in all slabs converge to zero. Conceptually, the solution is expressed as a series,

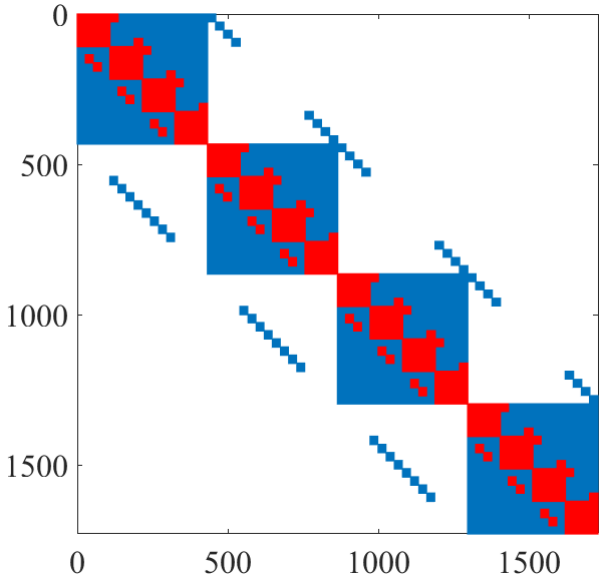

Figure 2. Sparsity pattern of the stiffness matrices in a $4\times4\times4$ domain. The global stiffness is in blue; the sub-domain matrices are in red.

$$\mathbf{a}_{n+1}=A^{-1}(F-B\mathbf{a}_n), \qquad (3)$$

However, the solution does not converge if the spectral radius of BA^{-1} is greater than 1. Inspiring by the Newton-Raphson method, a relaxation factor α can be provided to help establish convergence for possibly divergent Eqn. (3). The solution of the modified iterative scheme is expressed as,

$$\mathbf{a}_{n+1}=\alpha A^{-1}F+\left[(1-\alpha)\mathbf{I}-\alpha A^{-1}B\right]\mathbf{a}_n. \qquad (4)$$

Where $\mathbf{I}$ is the identity matrix. The relaxation factor α is chosen small enough to ensure the spectral radius of $(\alpha-1)\mathbf{I}+\alpha A^{-1}B$ be less than 1. The iterative scheme and the determination of the relaxation factor is expected to be discussed in more detailed in subsequent publications.

The parallel process is based on the iterative scheme. Either the angular decomposition (AD) or the domain decom-

position (DD) is used to partition the domain into n sub-domains [5]. Figure 3 illustrates the space and angle partitioning. For the AD method, as shown in Figure 3, the angular mesh is sliced into 4 sub-domains represented by 4 different patterns and assigned to 4 MPI processes, respectively. The processes solve the sub-domains individually, while a shared memory of accessing the information at each quadrature point is required to update the solutions for each iteration. For the DD method, the spatial mesh is divided into 4 sub-domains in different colors. The angular mesh in each sub-domain has to be same in order to communicate through processors. All the 4 sub-domains are assigned to a 4 MPI processes to solve the RTE in the sub-domains simultaneously. For each sub-domain interface, target values are the upstream values depending on the previous iteration from its neighbor sub-domain. In practice, after solving the RTE in the sub-domains, the solutions on the sub-domain interface are simply swapped. The iteration steps depend on the number of MPI processes. If 4 MPI processes are used, 3 iteration steps are required.

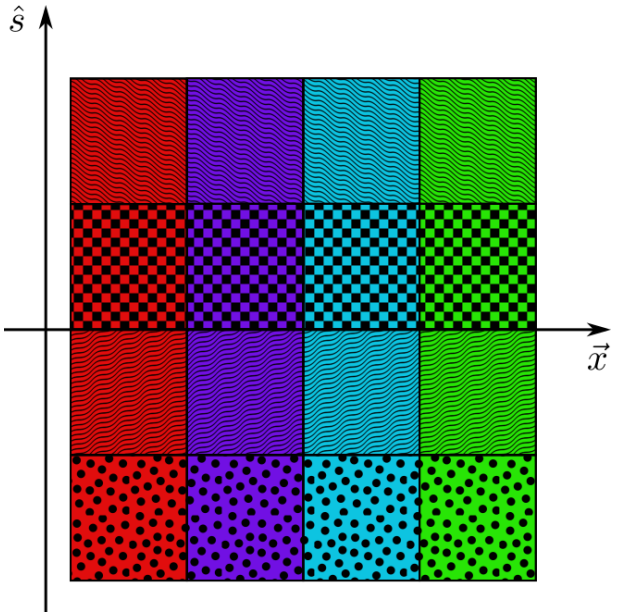

Figure 3. A schematic of the DD method and AD method.

5 Numerical examples

5.1 Code verification

Verification of the code is carried out using the Method of Manufactured Solution (MMS). In the MMS, an exact solution is given as an extra source term in the interior residual of the DG formulation. If the MS space belongs to the space of finite element solution. When the MS is a polynomial of order equal or less than that used to interpolate the trial solution, I, the exact solution is recovered. Otherwise, I asymptotically converges to the exact solution. Both direct and iterative 1D to 3D RTE solver are manage to capture or converge to the exact solution.

5.2 1D cylindrical example

According to Eqn. 2, the WRS of 1D cylindrical RTE, depending on r in space and the cosine of polar angle $\mu = \cos\theta$ and azimuthal angle $\tilde{\varphi}$ in angle, is derived by providing the formulation of $\mathrm{d}I(\mathbf{x},\hat{\mathbf{s}})/\mathrm{d}s = \sin\theta\cos\tilde{\varphi}\frac{\partial I(r,\mu,\tilde{\varphi})}{\partial r} - \frac{\sin\theta\sin\tilde{\varphi}}{r}\frac{\partial I(r,\mu,\tilde{\varphi})}{\partial\tilde{\varphi}}$, as mentioned Sec. 2.

In this example, inner and outer radii are $R_1 = 1$, $R_2 = 2$, $\beta = 1$, and $\sigma_s = 0.1$. $\Phi = 1$ corresponds to isotropic scattering. The inner surface is hot ($T_1 = 2000K$) and highly reflective ($\varepsilon_1 = 0.1$); the outer surface is relatively cool ($T_2 = 400K$) and is a strong absorber ($\varepsilon_2 = 0.9$). A $16\times16\times16$ grid with polynomial order $p = 1$ is used for the DG solution. For the iterative solver, the AD scheme is used to slice the domain in to 16 sub-domains, while only applied in μ direction to avoid additional interface communication in $\tilde{\varphi}$ direction. The result is shown in Figure 4. Compared to the direct solver, the iterative solver uses the memory 80% less than the direct solver.

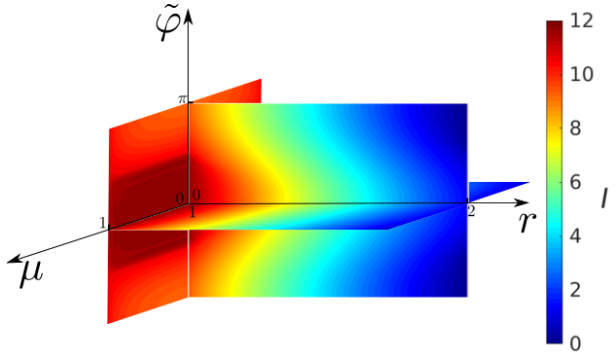

Figure 4. Contour plot of radiation intensity of the benchmark problem for $R_1/R_2 = 0.5$ and $\tau_2 - \tau_1 = 10$.

5.3 2D rectangular enclosure

A benchmark problem of an anisotropically scattering medium in a rectangular enclosure is investigated. The left hand side of the RTE, Eqn 1, in 2D Cartesian coordinate is written as,

$$\frac{\mathrm{d}I(\mathbf{x},\hat{\mathbf{s}})}{\mathrm{d}s} = \sqrt{1-\mu^2}\cos\varphi\frac{\partial I}{\partial x} + \sqrt{1-\mu^2}\sin\varphi\frac{\partial I}{\partial y}.$$

The size of the rectangle is 1×1. The isotropic incident radiation on the left boundary is $\bar{I} = 1$. The intensity remains 0 on the rest boundaries. The Rayleigh phase function is employed in this problem, where phase function $\Phi(\mu,\varphi,\mu',\varphi')$ is given,

$$\Phi(\mu,\varphi,\mu',\varphi') = \frac{3}{4}\left\{1+\left[\sqrt{(1-\mu^2)(1-\mu'^2)}\cos(\varphi-\varphi')+\mu\mu'\right]^2\right\}.$$

The extinction coefficient is $\beta = 1$. The scattering coefficient is $\sigma_s = 0.5$. The result is shown in Figure 5 in different directions.

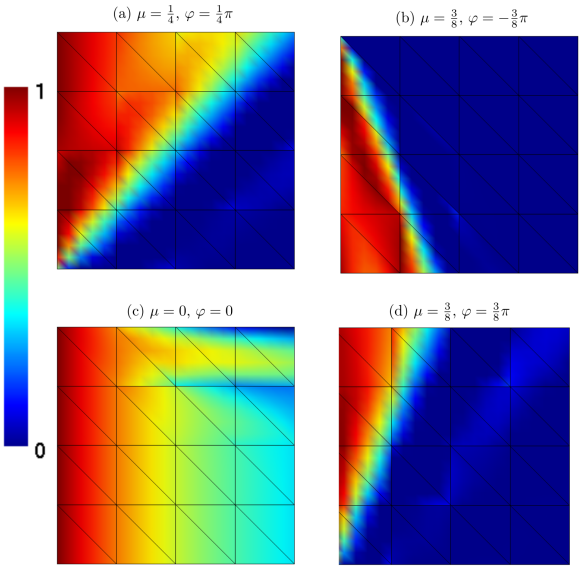

Figure 5. Contour plot of radiation intensity of the benchmark problem at four different directions.

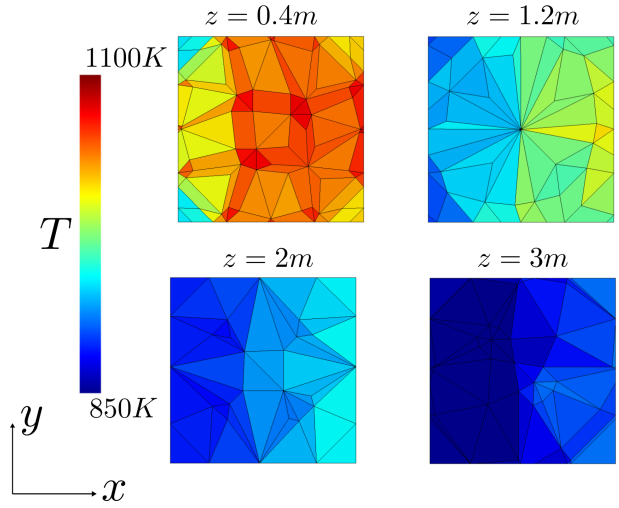

Figure 6. Contour plot of temperature field of the benchmark problem at the cross sections $z = 0.4m$, $z = 1.2m$, $z = 2m$, and $z = 3m$.

5.4 3D idealized furnace model

The left hand side of 3D RTE in Cartesian coordinate is,

$$\frac{\mathrm{d}I(\mathbf{x},\hat{\mathbf{s}})}{\mathrm{d}s} = \sqrt{1-\mu^2}\cos\varphi\frac{\partial I}{\partial x} + \sqrt{1-\mu^2}\sin\varphi\frac{\partial I}{\partial y} + \mu\frac{\partial I}{\partial z}.$$

A 3D idealized furnace model is conducted. The size of the rectangular cuboid is $2m \times 2m \times 4m$. The enclosure is filled with an absorbing-emitting medium with $\beta = \kappa = 0.5m^{-1}$. An additional heat source in the furnace is considered, $q = 5kW/m^3$. The boundary condition are $T_{(z=0)} = 1200K$, $T_{(z=4m)} = 400K$, other $T = 900K$. The solution is obtained using 563 tetrahedra spatial elements an extruded angular mesh 20×20 with polynomial order 0. The result is shown in Figure 6.

6 Conclusions

This paper has presented an iterative DG method for the numerical solution of the steady-state RTE from. The DG formulation is derived from the general RTE in both space and angle which can be easily derived in different coordinate systems and dimensions. The iterative solver significantly makes the stiffness matrix sparser, while remain the same accuracy as the direct solver. Moreover, the iterative scheme makes the parallel process easy to implement. Although the benchmark problem taken for examples are relatively simple, the benefits of our algorithm will be more pronounced for more complex problems.

7 Acknowledgements

This material is based upon work supported by the US Air Force Research Laboratory award number FA8650-14-D-1725-0007.

References

[1] William H Reed and TR Hill. Triangular mesh methods for the neutron transport equation. Technical report, Los Alamos Scientific Lab., N. Mex.(USA), 1973.

[2] S. Mudaliar, P.L. Clarke, and R. Abedi. Radiative transfer in turbulent flow using spacetime discontinuous Galerkin finite element method. In *Proceedings of 32nd International Union of Radio Science General Assembly & Scientific Symposium (URSI GASS)*, Palais des congres, Montreal, Canada, August 19-26, 2017.

[3] Philip Clarke, Hang Wang, Justin Garrard, Reza Abedi, and Saba Mudaliar. Space-angle discontinuous Galerkin method for plane-parallel radiative transfer equation. *Journal of Quantitative Spectroscopy and Radiative Transfer*, 233:87–98, 2019.

[4] H. Wang, R. Abedi, and S. Mudaliar. A discontinuous galerkin method for the solution of two dimensional axisymmetric radiative transfer problem. In *2019 USNC-URSI Radio Science Meeting (Joint with AP-S Symposium)*, pages 115–116, July 2019.

[5] M. A. Badri, P. Jolivet, B. Rousseau, and Y. Favennec. High performance computation of radiative transfer equation using the finite element method. *Journal of Computational Physics*, 360:74–92, 2018.